Role of Rac in controlling the actin cytoskeleton and chemotaxis in motile cells

Chang Y. Chung, Susan Lee, Celia Briscoe*, Charlene Ellsworth, and Richard A. Firtel†

Section of Cell and Developmental Biology, Division of Biology, Center for Molecular Genetics, University of California, San Diego, 9500 Gilman Drive, La Jolla, CA 92093-0634

Communicated by Dan L. Lindsley, Jr., University of California, San Diego, CA, February 17, 2000 (received for review November 1, 1999)

We have used the chemotactic ability of *Dictyostelium* cells to examine the roles of Rho family members, known regulators of the assembly of F-actin, in cell movement. Wild-type cells polarize with a leading edge enriched in F-actin toward a chemoattractant. Overexpression of constitutively active *Dictyostelium* Rac1B^{61L} or disruption of DdRacGAP1, which encodes a *Dictyostelium* Rac1 GAP, induces membrane ruffles enriched with actin filaments around the perimeter of the cell and increased levels of F-actin in resting cells. Whereas wild-type cells move linearly toward the cAMP source, Rac1B^{61L} and *Ddracgap1* null cells make many wrong turns and chemotaxis is inefficient, which presumably results from the unregulated activation of F-actin assembly and pseudopod extension. Cells expressing dominant-negative DdRac1B^{17N} do not have a well-defined F-actin-rich leading edge and do not protrude pseudopodia, resulting in very poor cell motility. From these studies and assays examining chemoattractant-mediated F-actin assembly, we suggest DdRac1 regulates the basal levels of F-actin assembly, its dynamic reorganization in response to chemoattractants, and cellular polarity during chemotaxis.

Dictyostelium | chemotaxis | Rac1 | F-actin

Chemotaxis, directed cell movement toward a chemoattractant agent, is involved in diverse biological responses, including wound healing in vertebrates, migration of tumor cells, metastasis of cancer cells, and aggregation leading to the formation of the multicellular organism in *Dictyostelium* (1–5). This process is activated by a large and diverse number of extracellular ligands that bind to cell surface receptors and leads to the directed reorganization of the actin and myosin cytoskeletons, pseudopod extension in the direction of the chemoattractant source, and cell movement via pathways that are thought to be highly conserved between mammals and *Dictyostelium* (3, 6–8). In polymorphonuclear leukocytes, macrophage, and *Dictyostelium* cells, chemotaxis can be mediated through G protein-coupled cell surface receptors, and in mammalian cells, the response is thought to function through G_i via release of $G\beta\gamma$ subunits (9–11). In *Dictyostelium*, the chemoattractants folic acid and cAMP (the chemoattractant that mediates aggregation) function through the folate receptor and cAMP receptor cAR1 via heterotrimeric G proteins containing the coupled $G\alpha$ subunits $G\alpha4$ and $G\alpha2$, respectively (3, 12, 13). In *Dictyostelium*, the second messenger cGMP, produced by receptor activation of guanylyl cyclase, plays an essential role in regulating changes in the actin and myosin cytoskeletons (14). Other components such as the *Dictyostelium* Akt/PKB, Ras protein RasG, the Ras exchange factor AleA, a MAP kinase cascade, a novel Ras-interacting protein RIP3, phosphatidyl inositol-3 kinase, and PAKa, a homologue of mammalian PAK1, are involved in different aspects of the signaling pathway that leads to cell movement and chemotaxis (2, 15–20). Transduction of the chemotactic signal to second messengers induces rearrangement of cytoskeletal components, including the focal nucleation and polymerization of actin at the leading edge and the relocalization of myosins (2, 21, 22).

The Rho family of small G proteins are key regulators of changes in the actin cytoskeleton (23–25). Constitutively active and dominant-negative forms of various Rho family members, including Rho, Rac, and Cdc42, elicit different effects on the actin cytoskeleton when microinjected into mammalian fibroblasts, including the formation of lamellipodia and filipodia and changes in stress fibers, and are able to induce cell motility in primary embryo fibroblasts (25). In yeast, Cdc42 is required for cell polarization and bud formation (26, 27), whereas a mutation in a putative Rac exchange factor leads to cell polarization defects during *Drosophila* embryogenesis (28). In macrophage, recent data from microinjection studies with dominant negative Rac1^{17N} and Cdc42^{17N} suggest that these proteins may play important but different roles in chemotaxis. Microinjection of Rac1^{17N} results in cells that are nonmotile, whereas injection of Cdc42^{17N} produces nonpolarized cells that lack directionality in cell movement in response to colony-stimulating factor-1 (29). Although significant advances in our understanding of the role of Rho family members in the regulation of the actin cytoskeleton derive from the analysis of stress fibers in nonmotile cells such as fibroblasts, these cells do not represent ideal models for the analysis of cell polarity and chemotaxis. In contrast, *Dictyostelium* cells provide a powerful system in which to identify and functionally dissect the cellular components controlling cell movement because of the ability to apply genetic and cell biological approaches. Because chemotaxis is required for aspects of morphogenesis and the aggregation stage of *Dictyostelium* development, the function of genes can be examined in their *in vivo* biological context.

We have taken advantage of the ability to readily analyze cell movement during chemotaxis in *Dictyostelium* to examine the role of Rho family members in the regulation of actin cytoskeleton rearrangements and chemotaxis *in vivo*. By using dominant forms of DdRac1B and a null mutation of a *Dictyostelium* Rac1 GAP, we demonstrate that DdRac1 plays a key role in regulating the basal level of F-actin assembly and the reorganization of the actin cytoskeleton in response to the chemoattractant cAMP.

Materials and Methods

Cell Culture and Development. The wild-type *Dictyostelium* cells, strain KAx-3, were grown and transformed by using standard techniques. *Dictyostelium* DdRac1B expression constructs were transformed with G418 as a selectable marker. Clonal isolates were selected on DM plates in association with *Escherichia coli* B/r carrying neomycin resistance. Morphology was examined by

Abbreviation: GBF, G-box binding factor.

*Present address: Department of Vascular Biology, Smithkline Beecham Pharmaceuticals, New Frontiers Science Park (North), Coldharbour Road, The Pinnacles, Harlow, Essex CM19 5AD, United Kingdom.

†To whom reprint requests should be addressed. E-mail: rafirtel@ucsd.edu.

The publication costs of this article were defrayed in part by page charge payment. This article must therefore be hereby marked "*advertisement*" in accordance with 18 U.S.C. §1734 solely to indicate this fact.

plating cells at different densities on nonnutrient agar plates containing 12 mM Na/KPO_4 (pH 6.1).

Molecular Biology. The DNA for DdRac1B was provided by S. Dharmawardhane (Scripps Research Institute, La Jolla, CA). Both DNAs were amplified by PCR, and an *Spe*I site followed by five A residues was added before the ATG translation initiation codon for cloning into and maximal expression from *Dictyostelium* expression vectors. Site-directed mutagenesis for creating constitutively active and dominant-negative mutants of DdRac1B was performed by using standard techniques. All constructs were confirmed by sequencing and expressed downstream from the *Act15* promoter.

DdRacGAP1 was disrupted by inserting the Bsr cassette in codon 394 and the construct, after digestion was transformed into *Dictyostelium* wild-type cells by electroporation. Clones carrying a gene disruption were identified by Southern and Northern blot hybridization of randomly selected colonies. Several null clones were examined and all showed indistinguishable phenotypes. One was selected for further analysis.

***In Vivo* Actin Polymerization Assay and Phalloidin Staining.** F-actin was quantified from tetramethylrhodamine B isothiocyanate-phalloidin staining of *Dictyostelium* cells as described in the study (4). Cells were pulsed with 30 nM cAMP at 6-min intervals for 5 h. Cells were diluted to 1×10^7 cells/ml and shaken at 200 rpm with 2 mM caffeine for 20 min. Cells were spun and resuspended with phosphate buffer [10 mM PO_4 buffer (pH 6.1)/2 mM $MgSO_4$] at 5×10^7 cells/ml and stimulated with 100 μM cAMP. Cells (500 μl) were taken at 5, 10, 20, 30, 50, and 80 s and mixed with actin buffer [20 mM KH_2PO_4/10 mM Pipes (pH 6.8)/5 mM EGTA/2 mM $MgCl_2$] containing 6% formaldehyde, 0.15% Triton X-100, and 1 μM tetramethylrhodamine B isothiocyanate phalloidin. Cells were fixed and stained for 1 h and spun down at $10{,}000 \times g$ for 5 min in the microcentrifuge. Pelleted cells were extracted with 1 ml of 100% methanol and fluorescence was measured (540 excitation/575 emission). To determine nonsaturable binding, 100 μM unlabeled phalloidin was included.

Phalloidin staining was done as described (2).

Aggregation-Competent Cells and the Chemotaxis Assay. Cells competent to chemotax toward cAMP (aggregation-competent cells) were obtained by pulsing cells in suspension for 5 h with 30 nM cAMP, conditions that maximally induce the expression of aggregation-stage genes required for aggregation, including the cAMP receptor cAR1 and the coupled G protein α subunit Gα2. The chemotaxis assays were done as described (2, 15). Cell movement was examined by tracing the movement of a single cell in a stack of images and analyzed by using DIAS software as described (2, 30, 31).

Results and Discussion

Disruption of DdRacGAP1 and Effect on F-actin Organization. To investigate the role of Rho family members in controlling cell movement, we disrupted the gene encoding the previously identified *Dictyostelium* Rho family member GAP DdRacGAP1 (32). RacGAP1 has an N-terminal Rac GAP domain immediately followed by a Src homology 3 (SH3) domain, central polyproline domains, and a *dbl* domain coupled with a PH domain located in the C-terminal one-third of the protein. The GAP domain of DdRacGAP1, expressed in bacteria, has the highest GTPase-stimulating activity for human RhoA and *Dictyostelium* Rac1A of the small G proteins tested (32). Rac1A, Rac1B, and Rac1C constitute the *Dictyostelium* Rac1 subfamily (33). Rac1A and Rac1B show >93% amino acid identity. The first 120 aa of the proteins are identical except for two conserved (I85V, S88A) aa substitutions. DdRacGAP1 transcripts are expressed during growth at a low level; expression then increases dramatically and is maximal during aggregation (4 and 8 h, data not shown). This expression pattern is similar to that of Rac1 (33).

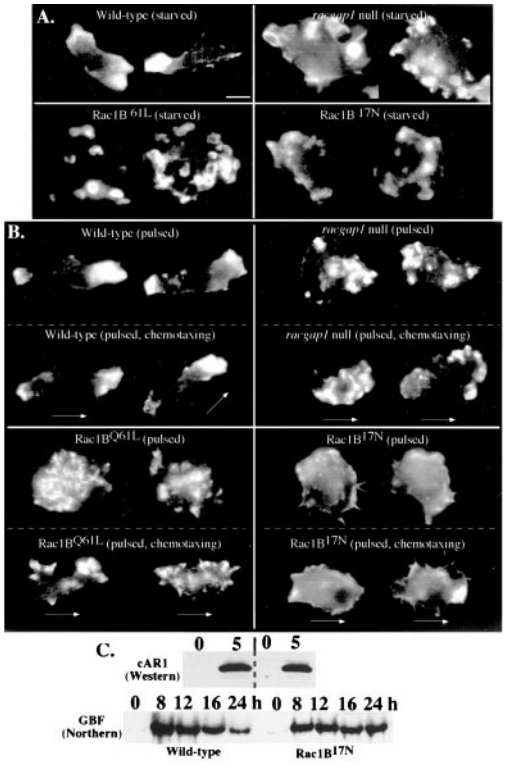

Fig. 1. DdRac1B activity controls the assembly and organization of the actin cytoskeleton of aggregation-stage cells and induction of gene expression. F-actin organization in cells lacking DdRacGAP1 or expressing constitutively active or dominant-negative mutants of DdRac1B was examined by FITC- or tetramethylrhodamine B isothiocyanate-labeled phalloidin staining. (*A*) Cells starved for 5 h. Wild-type cells have F-actin-rich lamellipodia at the leading edge and mutants have aberrant F-actin organization. (Bar = 5 μm.) (*B*) Cells pulsed for 5 h with 30 nM cAMP every 6 min (see legend to Fig. 3) and then either directly fixed or placed in a cAMP gradient established from a micropipette (see Fig. 3). Arrows show the direction of the micropipette containing cAMP and cell movement. (*C*) Expression of cAR1 protein and GBF transcripts in wild-type (KAx-3) cells and cells expressing DdRac1B^{17N}. For cAR1 expression, cells were pulsed for 5 h as described in *Materials and Methods*, the same conditions used for the chemotaxis assays. Cell lysates were run on a 10% SDS/PAGE gel and proteins were transferred to a membrane and blotted with anti-cAR1 polyclonal antibody, a gift of the Devreotes laboratory (Johns Hopkins University School of Medicine, Baltimore, MD). To examine GBF expression, total RNA was prepared from wild-type cells and cells expressing DdRac1B^{17N} at different stages of development on non-nutrient agar plates. RNA (6 μg) was loaded in each lane and probed with the GBF probe. t = 0 h, vegetative cells.

DdRacGAP1 was disrupted by homologous recombination (see *Materials and Methods*). RNA blot analysis showed that the disruption of *DdRacGAP1* resulted in a loss of transcripts from the gene (data not shown). *Ddracgap1* null strains exhibit no growth or cytokinesis defects (data not shown). Because mutant Rho family members have been demonstrated to affect the actin cytoskeleton, we used phalloidin staining of aggregation-stage cells (see *Materials and Methods*) to examine the distribution of F-actin in *Ddracgap1* null cells. Starved wild-type cells are well polarized and have F-actin-rich lamellipodia (pseudopodia) at the leading edge, and to a lesser degree, the retracting posterior cell body (Fig. 1*A*), as described (34, 35). In contrast, *Ddracgap1* null cells are less polarized but exhibit an up-regulated assembly of F-actin as evidenced by multiple, F-actin-enriched cortical

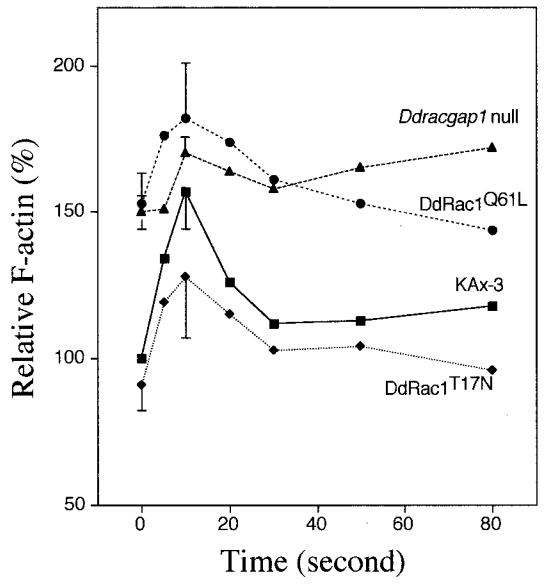

Fig. 2. F-actin polymerization responses on cAMP stimulation of *Dictyostelium* mutants. The F-actin content was determined by tetramethylrhodamine B isothiocyanate-phalloidin staining of cells fixed at various times after stimulation with 50 μM cAMP (see *Materials and Methods*). The amount of F-actin was normalized relative to the F-actin level of unstimulated wild-type cells (t = 0). Each data point represents the average of two or three independent measurements. Error bars are shown only at 0 and 10 s to avoid complexity.

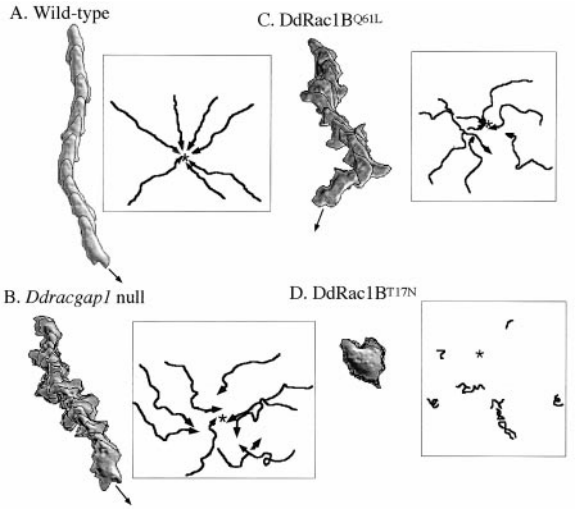

Fig. 3. Chemotactic movement of wild-type and mutant cells to a micropipette containing cAMP. Cells were pulsed with 30 nM cAMP at 6-min intervals for 5 h and cells were washed and resuspended in Na/KPO_4 buffer containing 200 μM $CaCl_2$ and $MgCl_2$. A small volume of cells were plated on glass-bottomed microwell plates (MarTek, Ashland, MA) and allowed to adhere to the surface for approximately 20 min. A micropipette filled with 100 μm cAMP was positioned and images of chemotaxing cells were captured every 6 s. The movement of cells and changes in cell shape were analyzed with the DIAS program, a newly developed image analysis system. Superimposed images representing cell shape at 1-min intervals are shown. Movement of cells during chemotaxis was traced and is presented in boxes. Wild-type cells are very polarized, their migration is rapid and directed toward the tip of the micropipette, and the vast majority of pseudopodia are extended only in the direction of the micropipette. The majority of *Ddracgap1* null cells move to the cAMP source, but they make many turns and lateral pseudopodia. Cells expressing $DdRac1B^{61L}$ show chemotactic defects similar to those of *Ddracgap1* null cells. Cell migration is severely impaired in cells expressing $DdRac1B^{17N}$. The star indicates the position of the cAMP source.

domains that include multiple lamellipodia and actin-enriched crowns, which may be macropinosomes (36). This is also seen as an elevated level of F-actin in unstimulated cells (Fig. 2). We expect that this unregulated increased F-actin assembly along the periphery of cells results from the unregulated activation of DdRac1.

To determine which domain(s) of DdRacGAP1 are required for its function, we expressed either the entire DdRacGAP1 or the various deletion mutations in the *Ddracgap1* null strain and examined the ability to complement the actin cytoskeletal and chemotaxis defects of *Ddracgap1* null cells. Only constructs that contained the N-terminal GAP and Src homology 3 (SH3) domains complemented the null phenotype, as determined by their ability to chemotax to cAMP, indicating that only these domains of the protein, and not the *dbl*-related domains, are required for proper actin cytoskeleton function in the biological contexts examined in these studies (data not shown).

Expression of Mutant Rac1B Proteins Leads to Different Effects on the Actin Cytoskeleton. We compared the phenotype of *Ddracgap1* null cells with the effects of expressing the dominant-negative and constitutively active form of DdRac1B. Like *Ddracgap1* null cells, cells expressing constitutively active $DdRac1B^{61L}$ exhibit a similar up-regulation in the assembly of F-actin in addition to multiple actin-enriched crowns in starved cells and aggregation-competent cells that have been pulsed for 5 h to maximally express cAMP receptors and other components of the signaling pathway as discussed below (Figs. 1 and 2). These data are consistent with RacGAP1 functioning as a GAP for DdRac1 family members *in vivo* as well as *in vitro* (32) and with the known ability of Rac to stimulate the formation of lamellipodia and membrane ruffles in mammalian fibroblasts *in vivo* (37). Because DdRacGAP1 has GAP activity against $DdRac1A^{(GTP)}$ *in vitro*, we expect that the *in vivo* changes in the actin cytoskeleton result from an elevated level of $DdRac1^{(GTP)}$ in *Ddracgap1* null cells. In contrast, starved and aggregation-stage cells expressing dominant-negative $DdRac1B^{17N}$ fail to polarize and lack F-actin-rich lamellipodia, suggesting a reduced activation of F-actin assembly in these cells (Figs. 1 and 2). This result suggests that dynamic regulation of F-actin assembly in $Rac1B^{17N}$-expressing cells might be significantly impaired. As shown below, *Ddracgap1* null cells and cells expressing $DdRac1B^{61L}$ can elongate on stimulation with cAMP in a chemotaxis assay (Fig. 3), but cells expressing dominant-negative $DdRac1B^{17N}$ do not.

To determine if there were changes in the actin cytoskeleton when cells are placed in a chemoattractant gradient, cells were placed on a cover slip and a micropipette containing cAMP was placed near the cells as described for the chemotaxis assay. As shown in Fig. 1*B*, wild-type cells are elongated and exhibit a strong polarized subcellular F-actin localization. F-actin levels are very high in the leading edge and are also enriched, but to a lesser degree, in the posterior of the cell. Little F-actin is found along the lateral sides of the cells. *Ddracgap1* null cells and cells expressing $DdRac1B^{61L}$ also become more elongated in chemoattractant gradients. However, they continue to exhibit multiple F-actin-enriched domains, representing multiple pseudopodia, around the periphery of the cell (Fig. 1*B*), which we expect is the result of unregulated, elevated F-actin assembly. Cells expressing $Rac1B^{17N}$ do not show dominant, F-actin-enriched domains, even when the cells are in a cAMP gradient (Fig. 1*B*).

We tested *Ddracgap1* null cells or cells expressing mutant DdRac1B for *in vivo* actin polymerization in response to cAMP stimulation. Wild-type cells show a rapid and transient increase in F-actin assembly (≈60–70%) 10 s after cAMP stimulation (Fig. 2), as described (7, 38–40). Consistent with our observation that *Ddracgap1* null cells exhibit an up-regulated assembly of F-actin in multiple cortical regions and have multiple actin-

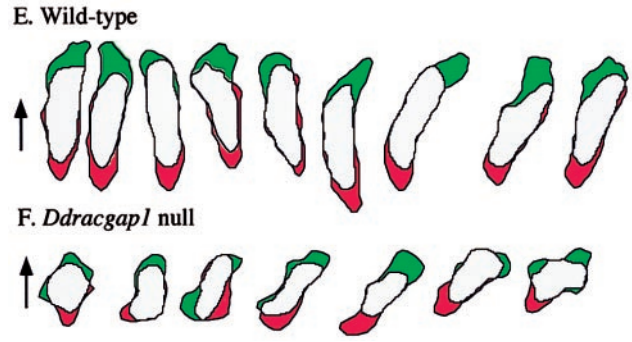

Fig. 4. Images at a 1-min interval of migrating wild-type and *Ddracgap1* null cells. Regions of the cell in the earlier picture that are not present in the later picture are shown in red. Regions of the cell in the later picture that are not present in the earlier picture are shown in green.

enriched crowns, the F-actin content in these cells before cAMP stimulation is significantly higher than that of wild-type cells. However, the F-actin polymerization response of these cells to cAMP is weaker than that of wild-type cells, with only a 10–20% increase in F-actin content. Cells expressing DdRac1B^{61L} have virtually the same F-actin polymerization response as *Ddracgap1* null cells. The F-actin level in unstimulated cells is also elevated, as expected from the up-regulated F-actin assembly. It is possible that the level of basal, unstimulated actin polymerization may be sufficiently high to preclude a robust stimulation by cAMP in *Ddracgap1* null cells and cells expressing DdRac1B^{61L}. It is also possible that DdRac1 must cycle between GDP- and GTP-bound states to regulate this response.

In contrast with DdRac1B^{61L} cells, cells expressing DdRac1B^{17N} exhibit a slightly lower level of F-actin assembly in unstimulated cells, but not as strikingly low as we observed in phalloidin staining. This finding might indicate that the assembled F-actin is more diffusely localized throughout the cell, a result that may not be observed by epifluorescence microscopy. Rac1B^{17N} cells still respond to cAMP, because they have an F-actin assembly peak with kinetics similar to those observed for wild-type cells. However, the peak level is significantly lower than that observed for wild-type cells, which is probably because of the dominant negative effect of Rac1B^{17N}. Combined with results from *Ddracgap1* null cells and DdRac1B^{61L} cells, this finding suggests that DdRac1 is involved in the dynamic regulation of F-actin assembly in response to a chemoattractant.

Role of DdRacGAP1 and Rac1B in the Regulation of Cell Motility During Chemotaxis. To test whether the changes in the actin cytoskeleton described above alter chemoattractant-induced cell migration, we used a chemotaxis assay combined with time-lapse video microscopy (Figs. 3 and 4). In this assay, the movement of aggregation-competent cells toward the chemoattractant cAMP emitted from a micropipette is recorded by using National Institutes of Health IMAGE software and analyzed with DIAS (Soltech, Oakdale, IA) image analysis software (see *Materials and Methods* for a description of aggregation-competent cells and the chemotaxis assay; refs. 2, 30, 31, and 41). To confirm that any chemotaxis defects that might be exhibited by any of the strains tested are not caused by an inability to respond to cAMP, we examined the level of the cAMP receptor cAR1 expressed in the aggregation-competent cells after pulsing (see *Materials and Methods*). As shown in Fig. 1*C*, Rac1B^{17N} cells exhibited a level of induced cAR1 receptor protein in Western blot analysis similar to that of wild-type cells. In addition, Rac1B^{17N} and wild-type cells exhibited a similar level of expression of the protein GBF (G-box binding factor), the developmentally regulated transcription factor essential for postaggregative development (42), when we plated the cells for development (Fig. 1*C*). Because GBF is maximally expressed in the mound stage, the slightly reduced level of GBF expression in Rac1B^{17N} cells plated for development is probably caused by the inefficient aggregate formation of this strain. *Ddracgap1* null and DdRac1B^{61L} cells have similar levels of cAR1 protein and GBF expression (data not shown).

As shown in Figs. 3 and 4 and summarized in Table 1, wild-type cells are very polarized (roundness, 51.7%), and their migration is rapid (speed, 10.06 μm/min) and directed toward the tip of the micropipette (directionality, 0.84). The vast majority of pseudopodia are extended only in the direction of the micropipette, and relatively few lateral pseudopodia form (Figs. 3*A* and 4; Table 1). The frequency of turning is very low in wild-type cells (average angle of directional change, 20.5°; Figs. 3*A* and 4; Table 1). *Ddracgap1* null cells also become polarized, but chemotax inefficiently because of random turns. As with wild-type cells, chemotaxis and the rate of cell migration is stimulated by the chemoattractant, but the rate of movement of *Ddracgap1* null cells (speed, 4.9 μm/min) is approximately half that of wild-type cells during chemotaxis. An analysis of the paths taken by individual cells indicates that most cells move toward the micropipette (Figs. 3*B* and 4). However, in contrast to wild-type cells, the movement is not linear toward the micropipette (directionality, 0.52) and cells make multiple false turns as they extend many lateral pseudopodia (10.3 pseudopodia per 10 min compared with 1.5 for wild-type cells; Table 1). We think these random pseudopodia result from uncontrolled activation of F-actin assembly along the periphery of cells because of the loss of DdRacGAP1 function, which is consistent with the F-actin staining in *Ddracgap1* null chemotaxing cells depicted in Fig. 1*B*. These random lateral pseudopodia result in greater directional changes, because the average directional change angle is 46°, more than double that of wild-type cells. A small fraction (≈5–10%) of the cells have migration pathways that appear to be independent of the direction of the chemoattractant source.

Table 1. Analysis of cell movement by using DIAS software

	Speed, μm/min	Directionality	Directional change, °	Roundness, %	Number of lateral pseudopodia per 10 min
Wild type	8.21 ± 1.81	0.85 ± 0.09	20.5 ± 5.8	51.7 ± 2.3	1.5 ± 0.5
Ddracgap1 null	4.9 ± 0.24	0.52 ± 0.04	46 ± 3.74	52 ± 1.2	10.3 ± 1.6
DdRac-1B^{Q61L}	3.22 ± 0.58	0.24 ± 0.16	70.2 ± 12	54 ± 7.9	8.62 ± 1.7
DdRac-1B^{T17N}	2.2 ± 0.25	0.012 ± 0.01	N/A	76.8 ± 13	N/A

Movement of cells was recorded by using National Institutes of Health IMAGE software (one image every 6 s). Cell movement was examined by tracing the movement of a single cell in a stack of images and analyzed by using DIAS software. Roundness is a measure (%) of how efficiently a given amount of perimeter encloses an area. A circle has the largest area for any given perimeter and has a roundness parameter of 100%. Generally, a more polarized cell shape produces less roundness. Directionality is the net path length divided by the total path length. This gives 1.0 for a completely straight path and a smaller value for a meandering path. Directional change represents the average angle of change in the direction of movement in each frame (6 s).

Because this strain is clonal and the phenotypes of this and other independently isolated *Ddracgap1* null strains or subclones are the same (data not shown), the reason that a small fraction of these cells have this behavior is presumably not because of heterogeneity in the population.

DdRac1B^{61L}-expressing cells have a chemotaxis phenotype similar to that of *Ddracgap1* null cells. The cells are mostly polarized in a chemotaxis gradient (roundness, 54%; Figs. 1*B* and 3*C*; Table 1). Although DdRac1B^{61L}-expressing cells chemotax, their migration is not as directed as that of wild-type cells (average directional change angle, 70.2°; Fig. 3*C* and Table 1), similar to our observations with *Ddracgap1* null cells. In addition, these cells often project pseudopodia laterally (8.63 per 10 min) as well as in the direction of the micropipette tip, which results in many false turns (directionality, 0.24) and slower migration (speed, 3.22 μm/min; Fig. 3*C* and Table 1). This may result from a nonspatially localized ("random") activation of downstream effectors along the plasma membrane. Although it is not proven, we expect that in wild-type cells, DdRac1B may be preferentially activated at the leading edge in response to ligand binding, as has been shown for the localization of the PH domain-containing proteins CRAC and Akt/PKB (15, 43). The fact that *Ddracgap1* null cells exhibit actin cytoskeletal and chemotactic defects similar to those of the DdRac1B^{61L}-expressing mutant cells suggests that DdRacGAP1 controls the *in vivo* levels of DdRac1B$^{(GTP)}$. False turns and inefficient cell movement caused by the unregulated F-actin assembly suggest that the spatial and temporal activity of Rac1B must be very tightly regulated to achieve the well-orchestrated F-actin regulation observed during chemotaxis.

In contrast, DdRac1B^{17N} cells fail to polarize (roundness, 77%) and essentially do not migrate (speed, 2.2 μm/min; Fig. 3*D* and Table 1). The cells appear to have a defect in pseudopod extension, consistent with the lack of F-actin-rich lamellipodia and membrane ruffles in these cells (Fig. 1*B*). This result is rather surprising because Rac1B^{17N} cells still exhibit a moderate F-actin polymerization response to cAMP stimulation (Fig. 2). It is possible that in DdRac1B^{17N} cells, the assembly of F-actin filaments might be insufficient in magnitude or improperly localized in the cell to provide a mechanical force for pseudopod protrusion. In addition, Rac1B may regulate cell polarization by pathways that do not directly involve F-actin polymerization. Localized activation of signaling pathways stimulating F-actin assembly at the leading edge and myosin II assembly in the rear cell body in response to a new chemoattractant gradient is a first step in resetting cell polarity and initiating chemotaxis in the direction of the new chemoattractant source. PAKa, a putative Rac1B effector, plays a key role in regulating myosin II assembly, which is important in defining axial polarity of the cell and biasing the direction of cell movement (2). The PAKa CRIB domain (Rac/Cdc42 binding domain) binds to Rac1B^{GTP}, implicating Rac1B in the regulation of cell polarity through the regulation of myosin II assembly in addition to controlling F-actin polymerization.

When cells expressing DdRac1B^{17N} are starved, plated on non-nutrient agar, and allowed to initiate multicellular development, aggregation is very delayed and many of the cells do not participate in aggregate formation, whereas DdRac1B^{61L} and *Ddracgap1* null cells aggregate with only slightly delayed kinetics when compared with wild-type cells (data not shown). The aggregation defect exhibited by DdRac1B^{17N} cells is not caused by the lack of responsiveness of the cells to cAMP, because cAMP receptor levels in all strains after pulsing are similar to those of wild-type cells (Fig. 1*C*; data not shown). This is consistent with the aggregation defect being the result of an impairment in the ability of these cells to move in response to chemoattractant signaling. Our results suggest that DdRac1B regulates cell migration by controlling the dynamics of F-actin assembly required for pseudopod protrusion and cell polarization, which is consistent with the observation that mammalian Rac1 plays an important role in macrophage migration (29).

Our results with DdRacGAP1 and DdRac1B are consistent with the previous suggestion that migration and orientation of *Dictyostelium* cells during chemotaxis are independently controlled (44). Our results with DdRac1B^{17N}-stably transformed *Dictyostelium* cells are completely consistent with observations when HsRac1B^{17N} was microinjected into macrophage (29). More recently, it has been found that Rac is essential for the protrusion of lamellipodia in migrating fibroblasts (25), which is also consistent with our results.

Conclusions

By analyzing cells lacking DdracGAP1 or expressing Rac1B mutants, we demonstrated that DdRac1B activity is important in F-actin regulation during chemotaxis. Our results suggest that the Rho family member DdRac1 controls the dynamic regulation of F-actin assembly during chemotaxis, and spatial and temporal control of Rac1 is required for the proper regulation of F-actin assembly and cell movement during chemotaxis. Our results agree with microinjection experiments in macrophage demonstrating that mammalian Rac1^{17N} blocks migration (29). We suggest that *Dictyostelium* DdRac1 regulates signaling pathways downstream from chemoattractant receptors that control aspects of cell movement, migration, and polarity.

We thank members of the R.A.F. lab for continued helpful suggestions during the course of this work, which was supported by grants from the U.S. Public Health Service to R.A.F.

1. Lahrtz, F., Piali, L., Spanaus, K. S., Seebach, J. & Fontana, A. (1998) *J. Neuroimmunol.* **85,** 33–43.
2. Chung, C. Y. & Firtel, R. A. (1999) *J. Cell Biol.* **147,** 559–575.
3. Chen, M. Y., Insall, R. H. & Devreotes, P. N. (1996) *Trends Genet.* **12,** 52–57.
4. Downey, G. P. (1994) *Curr. Opin. Immunol.* **6,** 113–124.
5. Hosaka, S., Suzuki, M. & Sato, H. (1979) *Gann* **70,** 559–561.
6. Chung, C. Y. & Firtel, R. A. (2000) in *Molecular Regulation*, ed. Means, P. M. & Conn, A. (Humana, Totowa, NJ), in press.
7. Zigmond, S. H., Joyce, M., Borleis, J., Bokoch, G. M. & Devreotes, P. N. (1997) *J. Cell Biol.* **138,** 363–374.
8. Parent, C. & Devreotes, P. (1999) *Science* **284,** 765–770.
9. Boulay, F., Naik, N., Giannini, E., Tardif, M. & Brouchon, L. (1997) *Ann. N.Y. Acad. Sci.* **832,** 69–84.
10. Cross, A. K., Richardson, V., Ali, S. A., Palmer, I., Taub, D. D. & Rees, R. C. (1997) *Cytokine* **9,** 521–528.
11. Neptune, E. R. & Bourne, H. R. (1997) *Proc. Natl. Acad. Sci. USA* **94,** 14489–14494.
12. Hadwiger, J. A. & Firtel, R. A. (1992) *Genes Dev.* **6,** 38–49.
13. Kumagai, A., Hadwiger, J. A., Pupillo, M. & Firtel, R. A. (1991) *J. Biol. Chem.* **266,** 1220–1228.
14. van Haastert, P. J. & Kuwayama, H. (1997) *FEBS Lett.* **410,** 25–28.
15. Meili, R., Ellsworth, C., Lee, S., Reddy, T. B. K., Ma, H. & Firtel, R. A. (1999) *EMBO J.* **18,** 2092–2105.
16. Ma, H., Gamper, M., Parent, C. & Firtel, R. A. (1997) *EMBO J.* **16,** 4317–4332.
17. Insall, R. H., Borleis, J. & Devreotes, P. N. (1996) *Curr. Biol.* **6,** 719–729.
18. Zhou, K., Pandol, S., Bokoch, G. & Traynor-Kaplan, A. E. (1998) *J. Cell Sci.* **111,** 283–294.
19. Tuxworth, R. I., Cheetham, J. L., Machesky, L. M., Spiegelmann, G. B., Weeks, G. & Insall, R. H. (1997) *J. Cell Biol.* **138,** 605–614.
20. Buczynski, G., Grove, B., Nomura, A., Kleve, M., Bush, J., Firtel, R. A. & Cardelli, J. (1997) *J. Cell Biol.* **136,** 1271–1286.
21. Spudich, J. A., Finer, J., Simmons, B., Ruppel, K., Patterson, B. & Uyeda, T. (1995) *Cold Spring Harbor Symp. Quant. Biol.* **60,** 783–791.
22. Eichinger, L., Lee, S. & Schleicher, M. (1999) *Microsc. Res. Tech.* **47,** 124–134.
23. Tapon, N. & Hall, A. (1997) *Curr. Opin. Cell Biol.* **9,** 86–92.
24. Hall, A. (1998) *Science* **279,** 509–514.
25. Nobes, C. D. & Hall, A. (1999) *J. Cell Biol.* **144,** 1235–1244.
26. Li, R., Zheng, Y. & Drubin, D. G. (1995) *J. Cell Biol.* **128,** 599–615.
27. Drubin, D. G. & Nelson, W. J. (1996) *Cell* **84,** 335–344.
28. Häcker, U. & Perrimon, N. (1998) *Genes Dev.* **12,** 274–284.

29. Allen, W. E., Zicha, D., Ridley, A. J. & Jones, G. E. (1998) *J. Cell Biol.* **141,** 1147–1157.
30. Wessels, D. & Soll, D. R., eds (1998) *Motion Analysis of Living Cells* (Wiley–Liss, New York), pp. 101–140.
31. Wessels, D., Voss, E., Von Bergen, N., Burns, R., Stites, J. & Soll, D. R. (1998) *Cell Motil. Cytoskel.* **41,** 225–246.
32. Ludbrook, S. B., Eccleston, J. F. & Strom, M. (1997) *J. Biol. Chem.* **272,** 15682–15686.
33. Bush, J., Franek, K. & Cardelli, J. (1993) *Gene* **136,** 61–68.
34. Gerisch, G., Albrecht, R., Heizer, C., Hodgkinson, S. & Maniak, M. (1995) *Curr. Biol.* **5,** 1280–1285.
35. Condeelis, J. (1993) *Annu. Rev. Cell Biol.* **9,** 411–444.
36. Hacker, U., Albrecht, R. & Maniak, M. (1997) *J. Cell Sci.* **110,** 105–112.
37. Ridley, A. J., Paterson, H. F., Johnston, C. L., Diekmann, D. & Hall, A. (1992) *Cell* **70,** 401–410.
38. Hall, A. L., Schlein, A. & Condeelis, J. (1988) *J. Cell. Biochem.* **37,** 285–299.
39. Hall, A., Warren, V. & Condeelis, J. (1989) *Dev. Biol.* **136,** 517–525.
40. Hall, A. L., Warren, V., Dharmawardhane, S. & Condeelis, J. (1989) *J. Cell Biol.* **109,** 2207–2213.
41. Lee, S., Parent, C. A., Insall, R. & Firtel, R. A. (1999) *Mol. Biol. Cell* **10,** 2829–2845.
42. Schnitzler, G. R., Fischer, W. H. & Firtel, R. A. (1994) *Genes Dev.* **8,** 502–514.
43. Parent, C. A., Blacklock, B. J., Froehlich, W. M., Murphy, D. B. & Devreotes, P. N. (1998) *Cell* **95,** 81–91.
44. Van Duijn, B. & Van Haastert, P. J. (1992) *J. Cell Sci.* **102,** 763–768.